1.5 GHz picosecond pulse generation from a monolithic waveguide laser with a graphene-film saturable output coupler

1.5 GHz picosecond pulse generation from a monolithic waveguide laser with a graphene-film saturable output coupler

Rose Mary,[1,*] Graeme Brown,[1] Stephen J. Beecher,[1] Felice Torrisi,[2] Silvia Milana,[2] Daniel Popa,[2] Tawfique Hasan,[2] Zhipei Sun,[2] Elefterios Lidorikis,[3] Seiki Ohara,[4] Andrea C. Ferrari,[2] and Ajoy K. Kar[1]

[1]*SUPA, Institute of Photonics and Quantum Sciences, School of Engineering and Physical Sciences, Heriot-Watt University, EH14 4AS, UK*
[2]*Cambridge Graphene Centre, University of Cambridge, Cambridge CB3 0FA, UK*
[3]*Department of Materials Science and Engineering, University of Ioannina, Ioannina, Greece*
[4]*Asahi Glass Co., Ltd. Research Center, 1150, Hazawa-cho, Kanagawa-ku, Yokohama, Kanagawa 221-8755, Japan*
[*]*rm330@hw.ac.uk*

Abstract: We fabricate a saturable absorber mirror by coating a graphene-film on an output coupler mirror. This is then used to obtain Q-switched mode-locking from a diode-pumped linear cavity channel waveguide laser inscribed in Ytterbium-doped Bismuthate Glass. The laser produces 1.06 ps pulses at ~1039 nm, with a 1.5 GHz repetition rate, 48% slope efficiency and 202 mW average output power. This performance is due to the combination of the graphene saturable absorber and the high quality optical waveguides in the laser glass.

OCIS codes: (230.7380) Waveguides, channeled; (140.3615) Lasers, ytterbium; (140.7090) Ultrafast lasers; (160.4236) Nanomaterials; (160.4330) Nonlinear optical materials.

References and links

1. T. Hasan, Z. Sun, F. Wang, F. Bonaccorso, P. H. Tan, A. G. Rozhin, and A. C. Ferrari, "Nanotube-polymer composites for ultrafast photonics," Adv. Mater. **21**(38â€“39), 3874–3899 (2009).
2. F. Bonaccorso, Z. Sun, T. Hasan, and A. C. Ferrari, "Graphene photonics and optoelectronics," Nat. Photonics **4**(9), 611–622 (2010).
3. Z. Sun, T. Hasan, and A. C. Ferrari, "Ultrafast lasers mode-locked by nanotubes and graphene," Physica E **44**(6), 1082–1091 (2012).
4. D. Popa, Z. Sun, T. Hasan, F. Torrisi, F. Wang, and A. C. Ferrari, "Graphene Q-switched, tunable fiber laser," Appl. Phys. Lett. **98**(7), 073106 (2011).
5. D. Popa, Z. Sun, T. Hasan, W. B. Cho, F. Wang, F. Torrisi, and A. C. Ferrari, "74-fs nanotube-mode-locked fiber laser," Appl. Phys. Lett. **101**(15), 153107 (2012).
6. Z. Sun, T. Hasan, F. Torrisi, D. Popa, G. Privitera, F. Wang, F. Bonaccorso, D. M. Basko, and A. C. Ferrari, "Graphene mode-locked ultrafast laser," ACS Nano **4**(2), 803–810 (2010).
7. Z. Sun, D. Popa, T. Hasan, F. Torrisi, F. Wang, E. Kelleher, J. Travers, V. Nicolosi, and A. Ferrari, "A stable, wideband tunable, near transform-limited, graphene-mode-locked, ultrafast laser," Nano Res. **3**(9), 653–660 (2010).
8. M. Zhang, E. J. R. Kelleher, F. Torrisi, Z. Sun, T. Hasan, D. Popa, F. Wang, A. C. Ferrari, S. V. Popov, and J. R. Taylor, "Tm-doped fiber laser mode-locked by graphene-polymer composite," Opt. Express **20**(22), 25077–25084 (2012).
9. J. Ma, G. Q. Xie, P. Lv, W. L. Gao, P. Yuan, L. J. Qian, H. H. Yu, H. J. Zhang, J. Y. Wang, and D. Y. Tang, "Graphene mode-locked femtosecond laser at 2 μm wavelength," Opt. Lett. **37**(11), 2085–2087 (2012).
10. L. M. Zhao, D. Y. Tang, H. Zhang, X. Wu, Q. Bao, and K. P. Loh, "Dissipative soliton operation of an ytterbium-doped fiber laser mode locked with atomic multilayer graphene," Opt. Lett. **35**(21), 3622–3624 (2010).
11. D. Popa, Z. Sun, F. Torrisi, T. Hasan, F. Wang, and A. C. Ferrari, "Sub 200 fs pulse generation from a graphene mode-locked fiber laser," Appl. Phys. Lett. **97**(20), 203106 (2010).
12. F. Wang, A. G. Rozhin, V. Scardaci, Z. Sun, F. Hennrich, I. H. White, W. I. Milne, and A. C. Ferrari, "Wideband-tuneable, nanotube mode-locked, fibre laser," Nat. Nanotechnol. **3**(12), 738–742 (2008).
13. G. Della Valle, R. Osellame, G. Galzerano, N. Chiodo, G. Cerullo, P. Laporta, O. Svelto, U. Morgner, A. G. Rozhin, V. Scardaci, and A. C. Ferrari, "Passive mode locking by carbon nanotubes in a femtosecond laser written waveguide laser," Appl. Phys. Lett. **89**(23), 231115 (2006).

#182934 - $15.00 USD Received 7 Jan 2013; revised 10 Mar 2013; accepted 13 Mar 2013; published 25 Mar 2013

14. S. J. Beecher, R. R. Thomson, N. D. Psaila, Z. Sun, T. Hasan, A. G. Rozhin, A. C. Ferrari, and A. K. Kar, "320 fs pulse generation from an ultrafast laser inscribed waveguide laser mode-locked by a nanotube saturable absorber," Appl. Phys. Lett. **97**(11), 111114 (2010).
15. A. A. Lagatsky, Z. Sun, T. S. Kulmala, R. S. Sundaram, S. Milana, F. Torrisi, O. L. Antipov, Y. Lee, J. H. Ahn, C. T. A. Brown, W. Sibbett, and A. C. Ferrari, "2μm Solid-State Laser Mode-locked By Single-Layer Graphene," Appl. Phys. Lett. **102**(1), 013113 (2013).
16. F. Bonaccorso, A. Lombardo, T. Hasan, Z. Sun, L. Colombo, and A. C. Ferrari, "Production and processing of graphene and 2d crystals," Mater. Today **15**(12), 564–589 (2012).
17. O. Okhotnikov, A. Grudinin, and M. Pessa, "Ultra-fast fibre laser systems based on SESAM technology: new horizons and applications," New J. Phys. **6**, 177 (2004).
18. U. Keller and E. Wolf, *Progress in Optics* (Elsevier, 2004).
19. D. Brida, A. Tomadin, C. Manzoni, Y. J. Kim, A. Lombardo, S. Milana, R. R. Nair, K. S. Novoselov, A. C. Ferrari, G. Cerullo, and M. Polini, "Ultrafast collinear scattering and carrier multiplication in graphene," arXiv:1209.5729 (2012).
20. C. Hönninger, R. Paschotta, F. Morier-Genoud, M. Moser, and U. Keller, "Q-switching stability limits of continuous-wave passive mode locking," J. Opt. Soc. Am. B **16**(1), 46–56 (1999).
21. R. W. Boyd, *Nonlinear Optics* (AP, 2008).
22. S. H. Chung and E. Mazur, "Surgical applications of femtosecond lasers," J Biophotonics **2**(10), 557–572 (2009).
23. S. Nolte, C. Momma, H. Jacobs, A. Tünnermann, B. N. Chichkov, B. Wellegehausen, and H. Welling, "Ablation of metals by ultrashort laser pulses," J. Opt. Soc. Am. B **14**(10), 2716–2722 (1997).
24. J. Mertz, "Nonlinear microscopy: new techniques and applications," Curr. Opin. Neurobiol. **14**(5), 610–616 (2004).
25. S. A. Diddams, "The evolving optical frequency comb," J. Opt. Soc. Am. B **27**(11), B51–B62 (2010).
26. M. P. Moreno and S. S. Vianna, "Femtosecond 1 GHz Ti:sapphire laser as a tool for coherent spectroscopy in atomic vapor," J. Opt. Soc. Am. B **28**(9), 2066–2069 (2011).
27. G. Della Valle, R. Osellame, and P. Laporta, "Micromachining of photonic devices by femtosecond laser pulses," J. Opt. A, Pure Appl. Opt. **11**(1), 013001 (2009).
28. A. Choudhary, A. A. Lagatsky, P. Kannan, W. Sibbett, C. T. A. Brown, and D. P. Shepherd, "Diode-pumped femtosecond solid-state waveguide laser with a 4.9 GHz pulse repetition rate," Opt. Lett. **37**(21), 4416–4418 (2012).
29. A. Martinez, K. Fuse, and S. Yamashita, "Mechanical exfoliation of graphene for the passive mode-locking of fiber lasers," Appl. Phys. Lett. **99**(12), 121107 (2011).
30. H. Yu, X. Chen, H. Zhang, X. Xu, X. Hu, Z. Wang, J. Wang, S. Zhuang, and M. Jiang, "Large energy pulse generation modulated by graphene epitaxially grown on silicon carbide," ACS Nano **4**(12), 7582–7586 (2010).
31. J. Liu, Y. G. Wang, Z. S. Qu, L. H. Zheng, L. B. Su, and J. Xu, "Graphene oxide absorber for 2 μm passive mode-locking Tm:$YAlO_3$ laser," Laser Phys. Lett. **9**(1), 15–19 (2012).
32. C. Mattevi, G. Eda, S. Agnoli, S. Miller, K. A. Mkhoyan, O. Celik, D. Mastrogiovanni, G. Granozzi, E. Garfunkel, and M. Chhowalla, "Evolution of electrical, chemical, and structural properties of transparent and conducting chemically derived graphene thin films," Adv. Funct. Mater. **19**(16), 2577–2583 (2009).
33. Y. Hernandez, V. Nicolosi, M. Lotya, F. M. Blighe, Z. Sun, S. De, I. T. McGovern, B. Holland, M. Byrne, Y. K. Gun'Ko, J. J. Boland, P. Niraj, G. Duesberg, S. Krishnamurthy, R. Goodhue, J. Hutchison, V. Scardaci, A. C. Ferrari, and J. N. Coleman, "High-yield production of graphene by liquid-phase exfoliation of graphite," Nat. Nanotechnol. **3**(9), 563–568 (2008).
34. T. Hasan, F. Torrisi, Z. Sun, D. Popa, V. Nicolosi, G. Privitera, F. Bonaccorso, and A. C. Ferrari, "Solution-phase exfoliation of graphite for ultrafast photonics," Phys. Status Solidi B **247**(11-12), 2953–2957 (2010).
35. A. C. Ferrari, J. C. Meyer, V. Scardaci, C. Casiraghi, M. Lazzeri, F. Mauri, S. Piscanec, D. Jiang, K. S. Novoselov, S. Roth, and A. K. Geim, "Raman spectrum of graphene and graphene layers," Phys. Rev. Lett. **97**(18), 187401 (2006).
36. A. C. Ferrari and J. Robertson, "Interpretation of Raman spectra of disordered and amorphous carbon," Phys. Rev. B **61**(20), 14095–14107 (2000).
37. C. Casiraghi, A. Hartschuh, H. Qian, S. Piscanec, C. Georgi, A. Fasoli, K. S. Novoselov, D. M. Basko, and A. C. Ferrari, "Raman spectroscopy of graphene edges," Nano Lett. **9**(4), 1433–1441 (2009).
38. A. C. Ferrari and J. Robertson, "Resonant Raman spectroscopy of disordered, amorphous, and diamondlike carbon," Phys. Rev. B **64**(7), 075414 (2001).
39. S. Latil, V. Meunier, and L. Henrard, "Massless fermions in multilayer graphitic systems with misoriented layers: Ab initio calculations and experimental fingerprints," Phys. Rev. B **76**(20), 201402 (2007).
40. A. Das, S. Pisana, B. Chakraborty, S. Piscanec, S. K. Saha, U. V. Waghmare, K. S. Novoselov, H. R. Krishnamurthy, A. K. Geim, A. C. Ferrari, and A. K. Sood, "Monitoring dopants by Raman scattering in an electrochemically top-gated graphene transistor," Nat. Nanotechnol. **3**(4), 210–215 (2008).
41. D. M. Basko, S. Piscanec, and A. C. Ferrari, "Electron-electron interactions and doping dependence of the two-phonon Raman intensity in graphene," Phys. Rev. B **80**(16), 165413 (2009).
42. M. Lotya, Y. Hernandez, P. J. King, R. J. Smith, V. Nicolosi, L. S. Karlsson, F. M. Blighe, S. De, Z. Wang, I. T. McGovern, G. S. Duesberg, and J. N. Coleman, "Liquid phase production of graphene by exfoliation of graphite in surfactant/water solutions," J. Am. Chem. Soc. **131**(10), 3611–3620 (2009).
43. V. G. Kravets, A. N. Grigorenko, R. R. Nair, P. Blake, S. Anissimova, K. S. Novoselov, and A. K. Geim, "Spectroscopic ellipsometry of graphene and an exciton-shifted van Hove peak in absorption," Phys. Rev. B **81**(15), 155413 (2010).

#182934 - $15.00 USD Received 7 Jan 2013; revised 10 Mar 2013; accepted 13 Mar 2013; published 25 Mar 2013

44. K. F. Mak, M. Y. Sfeir, Y. Wu, C. H. Lui, J. A. Misewich, and T. F. Heinz, "Measurement of the optical conductivity of graphene," Phys. Rev. Lett. **101**(19), 196405 (2008).
45. Z. Q. Li, E. A. Henriksen, Z. Jiang, Z. Hao, M. C. Martin, P. Kim, H. L. Stormer, and D. N. Basov, "Dirac charge dynamics in graphene by infrared spectroscopy," Nat. Phys. **4**(7), 532–535 (2008).
46. M. Haiml, R. Grange, and U. Keller, "Optical characterization of semiconductor saturable absorbers," Appl. Phys. B **79**(3), 331–339 (2004).
47. W. B. Cho, J. W. Kim, H. W. Lee, S. Bae, B. H. Hong, S. Y. Choi, I. H. Baek, K. Kim, D.-I. Yeom, and F. Rotermund, "High-quality, large-area monolayer graphene for efficient bulk laser mode-locking near 1.25 μm," Opt. Lett. **36**(20), 4089–4091 (2011).
48. Y. Nasu, M. Kohtoku, and Y. Hibino, "Low-loss waveguides written with a femtosecond laser for flexible interconnection in a planar light-wave circuit," Opt. Lett. **30**(7), 723–725 (2005).
49. R. Mary, S. J. Beecher, G. Brown, R. R. Thomson, D. Jaque, S. Ohara, and A. K. Kar, "Compact, highly efficient ytterbium doped bismuthate glass waveguide laser," Opt. Lett. **37**(10), 1691–1693 (2012).
50. M. Bass and E. W. Van Stryland, *Fiber Optics Handbook: Fiber, Devices, and Systems for Optical Communications* (McGraw-Hill, 2002).
51. D. V. Linde, "Characterization of the noise in continuously operating mode-locked lasers," Appl. Phys. B **39**(4), 201–217 (1986).

1. Introduction

Carbon nanotubes (CNTs) and graphene have emerged as promising saturable absorbers (SA) for a variety of applications [1–3], opening a new phase in the development of passively Q-switched [4] and mode-locked lasers [5–15]. While the predominantly used semiconductor saturable absorber mirrors (SESAMs) are limited by their narrow wavelength range [17], and complex fabrication [18], CNTs and graphene have simple, cost-effective production and integration [1–16]. Broadband operation is achieved with CNTs by combining tubes of different diameters [12]. However, for a particular wavelength, only CNTs in resonance are used, the remaining tubes contributing non-saturable losses [5]. Graphene has an inherent ultra-wide spectral range due to the linear dispersion of the Dirac electrons [1–4, 6, 7]. This, along with the ultrafast recovery time [19], and low saturation fluence [6, 11], makes it an excellent broadband SA [1, 6–8, 10, 11].

Under certain conditions, the saturable absorber can lead to a regime of Q-switched mode-locking (QML), where the laser output consists of mode-locked pulses of varying amplitudes within a Q-switched envelope [20]. This arises due to an interplay between the saturation effects in the SA, and, the gain medium favouring higher pulse energies with lower round trip losses. Q-switching instabilities in the cavity are also influenced by the long (*i.e.,* >1 μs) upper state lifetimes of the gain media in solid state lasers [20]. These lasers are useful for applications where the pulse energy stored within the gain medium is valuable [20], such as nonlinear frequency conversion [21], medical applications [22], and micromachining [23]. With the emerging trend in miniaturization of optical devices based on integration on-chip, the development of ultrafast lasers requires a complementary balance between device compactness and performance [13, 14]. Ultra-compact high repetition rate (>1 GHz) lasers are very useful for applications such as nonlinear microscopy [24], frequency combs [25] and spectroscopy [26]. The ease of SA integration into a compact cavity plays an important role [13, 14]. Lasers employing a waveguide cavity allow device compactness, meanwhile emulating the advantages of fiber lasers, such as high beam quality [17] and efficient heat dissipation [13, 14, 17]. Of the numerous methods available for waveguide fabrication, a simple yet reliable technology is ultrafast laser inscription (ULI), which utilizes ~100 fs focused pulses to induce permanent modifications within a substrate [27]. Mode-locked ULI waveguide lasers have been demonstrated using CNT-SAs [13, 14]; however, the fiber ring cavity did not allow miniaturization, thus high repetition rates.

Here we report pulse generation in a compact, ULI based waveguide laser in Ytterbium-doped Bismuthate Glass (Yb: BG), by using a graphene film (GF) transferred to an output coupler (OC) mirror as a SA. We achieve mode-locked pulses with 1.5 GHz repetition rate and 202 mW average output power, with 48% slope efficiency and 38% optical-to-optical conversion efficiency. The pulse duration is ~1.06 ps. The slope efficiency is high compared to that typical of monolithic pulsed waveguide lasers (*e.g.,* 27% [28]).

#182934 - $15.00 USD Received 7 Jan 2013; revised 10 Mar 2013; accepted 13 Mar 2013; published 25 Mar 2013

A variety of approaches have been used to make graphene-based SAs. For example, graphene-polymer composites, fabricated from dispersions produced by liquid phase exfoliation (LPE) of graphite [16], have been used to mode-lock fiber lasers at 1.5 [1, 7, 11] and 2 μm [8]. Films grown by chemical vapour deposition (CVD) [16] with 1 layer [15], 1-2 layers [9], and non-uniform multi-layers [10], have been used to mode-lock solid-state lasers at 2 μm [9, 15] and fiber lasers at 1 μm [10]. Reference [29]. used flakes produced by micromechanical exfoliation, with 4-40 layers, for mode-locking of fiber lasers at 1.5 μm. LPE graphene-polymer composites [4], and flakes (10-40 layers) grown by carbon segregation on SiC [16, 30], have been used for Q-switching of fiber lasers at 1.5 μm and solid-state lasers at 1 μm. Graphene oxide (GO) [16] was also used as SA, either as a film in solid-state lasers at 2 μm [31], or as composite in fiber lasers at 1.5 μm [2]. However, GO is an insulating material with many defects and gap states [16, 32], and may not offer the wideband tunability of graphene. Flakes grown by carbon segregation and CVD graphene require high substrate temperatures [9, 15, 16, 31], followed by transfer to the target substrate [9, 10, 15, 16]. Micromechanically exfoliated graphene has high structural and electronic quality [2, 16], but is limited in terms of yield, thus impractical for large-scale applications [16]. LPE has the advantage of scalability, room temperature processing and high yield, and does not require any growth substrate [16]. Dispersions produced by LPE can easily be embedded into polymers composites and integrated into various systems [2, 16]. Here we adopt a novel approach and use LPE graphene in a polymer-free film. This reduces non-saturable losses making it suitable for high average-power applications and device miniaturization.

2. Fabrication of the graphene film

The GF-SA is prepared as follows. Graphite flakes (Sigma Aldrich) undergo LPE [33] and are dispersed in deionised water with sodium deoxycholate, as for [6, 8]. High Resolution Transmission Electron Microscopy (HRTEM), Optical and Raman Spectroscopy are then used to characterize the dispersion. HRTEM shows that the sample consists of ~26% single-, ~22% bi- and ~18% tri-layers [8, 34], with ~1 μm average size. The dispersion then undergoes vacuum filtration via 25 nm pore-size filters. This blocks the flakes, while allowing water to pass through, resulting in a GF. This is then placed on an OC mirror, to be used in the laser, and on a quartz plate, for optical characterization, by applying pressure and heat (~80°C, to improve adhesion) for two hours, followed by dissolution of the filter in acetone. The resulting film is ~45 nm thick, as determined by profilometry. Its density is ~0.72 gcm^{-3}, derived by the weight (measured with a microbalance) of the filter before and after the GF deposition. This is ~1/3 of the density of bulk graphite.

Raman spectra are acquired at 457, 514, and 633 nm using a Renishaw InVia micro-Raman spectrometer. Figure 1(a) plots a typical Raman spectrum of the flakes in the dispersion. Besides the G and 2D peaks, significant D and D′ bands are also present [35, 36]. We assign the D and D' peaks to the sub-micrometer edges of our flakes [37], rather than to a large amount of disorder within the flakes. This is supported by the G peak dispersion, Disp(G) = 0.02 $cm^{-1}nm^{-1}$, much lower than in disordered carbons [38]. Figure 1(b) plots the GF Raman spectrum at 514 nm. Similar to the individual flakes discussed above, Disp(G) is 0.02 $cm^{-1}nm^{-1}$ [38]. The 2D peak is still single Lorentzian, but ~24 cm^{-1} larger than that of the individual flakes. Thus, even if the flakes are multi-layers, they are electronically decoupled and, to a first approximation, behave as a collection of single layers [34, 39]. We note that the ratio of the 2D and G integrated areas, A(2D)/A(G), is at most ~2, thus we estimate a doping ~$1.3x10^{13}$ cm^{-2} [41], i.e. a Fermi level shift ~4-500 meV [40, 41].

#182934 - $15.00 USD Received 7 Jan 2013; revised 10 Mar 2013; accepted 13 Mar 2013; published 25 Mar 2013

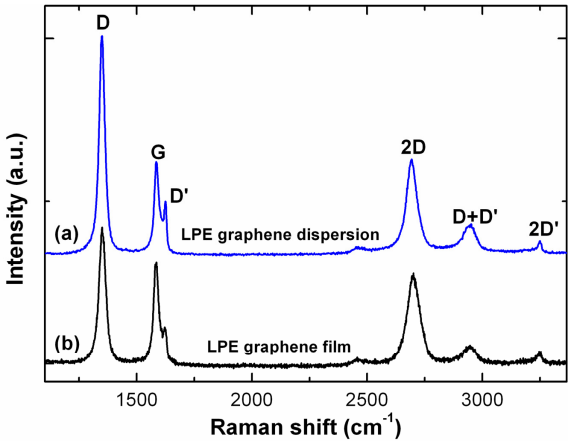

Fig. 1. Raman spectra measured at 514 nm of (a) graphene dispersion in SDC-Water and (b) graphene film.

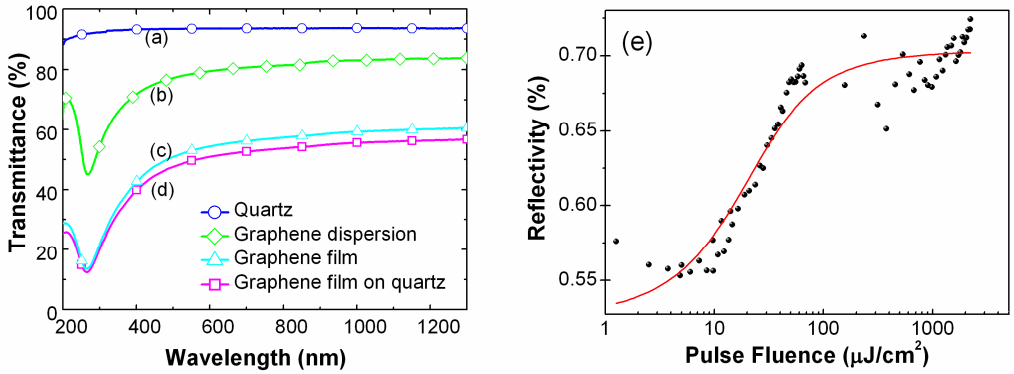

Fig. 2. Transmittance of (a) Quartz, (b) Graphene dispersion, (c) Graphene-film, and (d) Graphene-film on quartz. (e) Nonlinear reflectivity vs pulse fluence for the GF-SA.

Figure 2(b) plots the transmittance (T) of the graphene dispersion (diluted to 10% to avoid scattering losses at higher concentrations). Using $T = e^{-\alpha lc}$ where l[m] is the light path length, c[gL^{-1}] is the concentration of dispersed graphitic material, and α[$Lg^{-1}m^{-1}$] is the absorption coefficient, with α ~1390 $Lg^{-1}m^{-1}$ at 660 nm [42], we derive c ~0.18 gL^{-1}. The peak ~266 nm is a signature of the van Hove singularity in the graphene density of states [43]. Figures 2(a), 2(c), 2(d) plot the T of quartz (T_{Quartz}), GF (T_{GF}) and GF on quartz ($T_{GFQuartz}$). T_{GF} is derived from = $T_{GFQuartz}/T_{Quartz}$. The transmittance and reflectance of the GF at 1039 nm (the laser wavelength) are ~59% and ~11% respectively. To estimate the number of graphene layers from these measurements we use the recurrent matrix method. We calculate the reflectivity of an equivalent doped (~500 meV) graphite-like film as a function of the number of layers. In this model, the GF is approximated as a multilayered graphene film on a quartz substrate. The overall reflectivity of the film is calculated by evaluating the contributions of multiple reflections in the multilayer. We also include the correction to the graphene optical conductivity induced by doping [44]. While pristine graphene absorbs 2.3% per layer, doping, and consequent Pauli blocking, can significantly decrease this [6, 45]. By comparing our calculations with the data at 1039 nm we estimate that an 11% reflectivity translates to ~40 layers for our GF. Taking into account that its density is ~1/3 of graphite, this number of layers corresponds to an overall thickness ~40 nm, in good agreement with that measured by profilometry. We note that a 40 nm thick undoped and compact GF would absorb ~100% of the incident light and be near impossible to saturate, thus the low density and doping of our

#182934 - $15.00 USD Received 7 Jan 2013; revised 10 Mar 2013; accepted 13 Mar 2013; published 25 Mar 2013

film are essential for the SA to work. The nonlinear reflectivity of our GF is measured by using an ytterbium fiber laser system at 1064 nm, with a ~350 fs pulse duration. The characteristic curve is shown in Fig. 2(e) and yields a 10.2 μJ/cm^2 saturation fluence, a 17.6% modulation depth and a 30% non-saturable loss, using the model derived in [46]. The modulation depth of our GF is much larger than that reported for single-layer graphene based devices (e.g., 0.54% in [47].).

3. Waveguide laser fabrication and characterization

Figure 3 is the schematic of our laser cavity. We use a 50 mm Yb: BG substrate with 1.6 × 10^{26} m^{-3} Yb^{3+} dopants and 2.03 refractive index as gain medium. The waveguide is inscribed by focusing the pulses, through a 0.4 NA lens, 200 μm below the substrate surface, by a master oscillator power amplifier fiber laser (IMRA FCPA μ-Jewel D400) delivering 350 fs pulses at 1047 nm and 1 MHz repetition rate. An automated x-y-z stage translates the sample, thus extending the positive index change at the laser focus to form a waveguide. Low insertion loss waveguides with symmetric cross-sections are realized using a multi-scan technique [48], inscribed with pulse energies ~50 nJ. Previously, highly efficient cw lasing with 79% slope efficiency was demonstrated from the waveguide inscribed at a 8 mms^{-1} translation speed. The waveguide laser mode diameters are 8.88 and 8.75 μm in the horizontal and vertical axis, giving a 0.61 x 10^{-6} cm^2 laser mode area [49], and NA = 0.08.

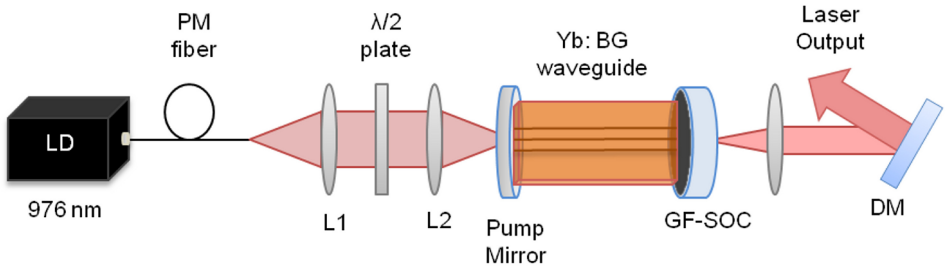

Fig. 3. Laser schematic. L1 and L2: Coupling lenses; PM: Polarization maintaining fiber; GF-SOC: Graphene-film saturable output coupler; DM: Dichroic mirror.

The pump source is a polarization-maintaining fiber-coupled diode laser at 976 nm, with 530 mW maximum pump power, and an angle cleaved fiber to avoid back reflections. Two identical lenses with a 6.2 mm focal length collimate and then refocus the pump light efficiently into the waveguide. A half-wave plate allows control of the plane of the pump polarization. A dichroic mirror with 99% reflectivity from 1010 to 1200 nm and less than 2% at the pump wavelength is used as the pump input mirror. The cavity mirrors are butt-coupled to waveguide ends using index matching gel, which reduces Fresnel reflections at the interfaces [50]. A dielectric mirror with a 60% reflectivity at the laser wavelength, and comparable to the optimum coupling for the waveguide laser [49], is chosen as the OC for the deposition of the GF. The laser output is collimated by a lens before a dichroic mirror separates the QML output from the residual pump light.

The laser operation initiates abruptly at a threshold pump power of 100 mW in a self-starting QML regime. The cavity is optimized by adjusting the pump coupling efficiency, pump beam polarization, and GF-SA position and angle. The mode area on the GF-SA is dictated by that of the waveguide. Using a fast photodiode (Thorlabs SIR5-FC) and a 50 GHz Bandwidth Agilent Infiniium DCA 86100A Oscilloscope, the initial repetition rate of the Q-switched envelope is measured as 200 kHz, with 17 mW average output power. Figure 4(a) shows the Q-switched envelope pulse repetition rate and energy evolution within a single Q-switched envelope. As the launch pump power is increased, the period between the Q-switched pulses reduces, indicating a tendency towards CW mode-locking. At the highest available pump power of 530 mW, the Q-switching modulation has a 0.95 MHz frequency

#182934 - $15.00 USD Received 7 Jan 2013; revised 10 Mar 2013; accepted 13 Mar 2013; published 25 Mar 2013

and a 202 mW average output power, corresponding to 220 nJ within each envelope. This is distributed along the mode-locked pulses existing within the Q-switched envelope. Figure 4(b) shows the mode-locked pulse train behaviour measured on a timescale of 500 ps/div. Mode-locked pulses at a 1.514 GHz fundamental repetition rate, corresponding to the free spectral range of the cavity, are measured within the Q-switched envelope. Mode-locking at the fundamental repetition rate is also verified by measuring the RF spectrum with a Rigol DSA 1030 spectrum analyser, Fig. 5(a). The ~4.2 MHz spectral width indicates the absence of pure CW mode-locking [51], as further shown in the inset of Fig. 5(a).

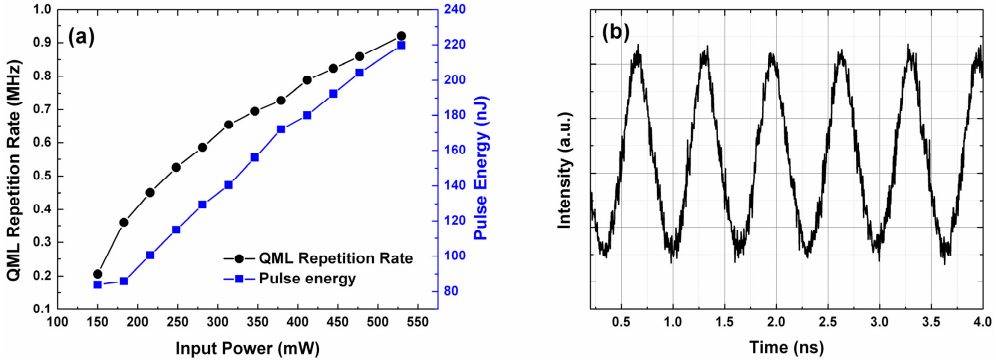

Fig. 4. (a) Repetition rate and energy within the Q-switched envelope, as a function of input pump power. (b) Mode-locked pulse train

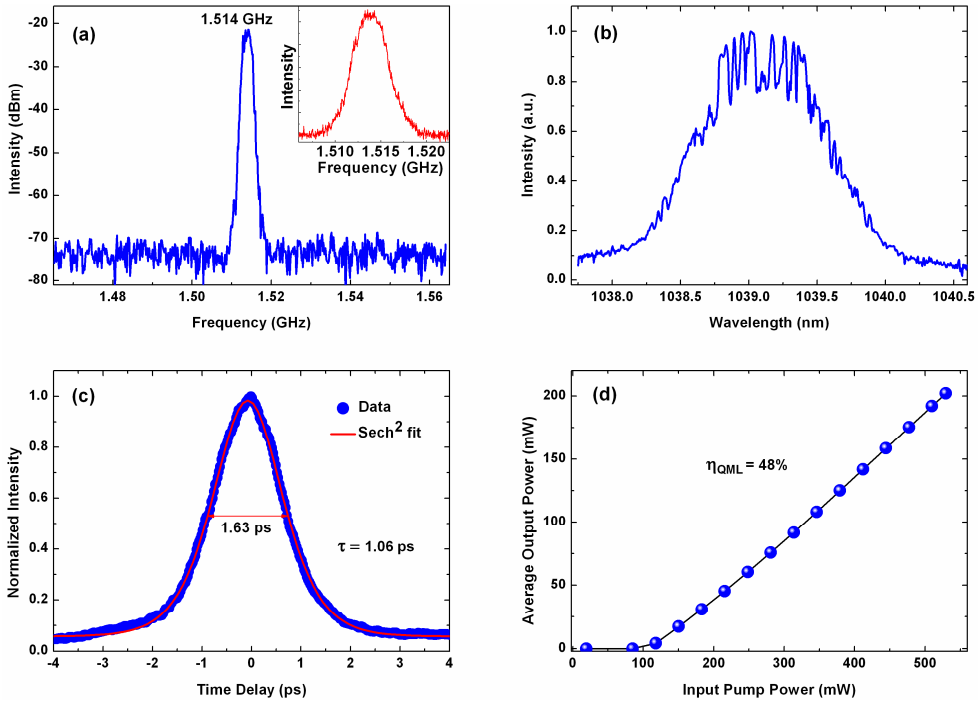

Fig. 5. (a) RF Spectrum measured at the maximum pump (zoom-out in the inset). (b) Corresponding optical spectrum. (c) Output autocorrelation trace. (d) Output power with launched pump power (with a slope efficiency of ~48% and a maximum output power of 202 mW).

The waveguide laser performance regime is determined by applying the criterion for stable continuous wave mode-locking derived in [20]: $E_p^2 > E_{sat.L}.E_{sat,A}.\Delta R$, where E_p is the

#182934 - $15.00 USD Received 7 Jan 2013; revised 10 Mar 2013; accepted 13 Mar 2013; published 25 Mar 2013

intracavity pulse energy, $E_{sat,L}$ the saturation energy of the gain medium, $E_{sat,A}$ the SA saturation energy, and ΔR the modulation depth. The experimentally derived saturation fluence and modulation depth of our GF-SA yield a QML parameter 2 orders of magnitude higher than that required for stable cw mode-locking, in agreement with the observed waveguide laser characteristics.

The optical spectrum is given in Fig. 5(b). The spectral bandwidth, corresponding to a pump power of 530 mW, is 1.1 nm. With increasing pump, the spectral peak migrates slightly to longer wavelengths. The intensity autocorrelation trace of the output pulse is plotted in Fig. 5(c). The temporal profile of the pulse is represented by a sech^2, giving a 1.06 ps pulse duration after deconvolution. For the 1039 nm output wavelength, the calculated time-bandwidth product is ~0.324, indicating the pulses to be near-transform-limited. For the maximum input pump power of 530 mW, we have an average output power of 202 mW. The average output power dependence on the pump is given in Fig. 5(d). The QML waveguide laser has a high slope efficiency of 48%, and a 38% overall optical-to-optical conversion efficiency. Stable QML pulses are observed over ~24 hours, demonstrating the good quality of the GF-SA and its resistance to damage.

4. Conclusion

We demonstrated a monolithic waveguide laser with stable and efficient Q-switched mode-locking using a graphene film placed on an output coupler. The ~40 nm film behaves like a collection of a few single layers of graphene by virtue its low density and doping, thus making it an effective saturable absorber. The easy integration of the saturable output coupler into the waveguide cavity, the compactness and reliability achieved therewith, and the superior laser performance marks a vital step in the development of compact ultrafast waveguide lasers fabricated using ultrafast laser inscription.

Acknowledgments

We acknowledge funding from ERC Grant NANOPOTS, EPSRC Grants EP/G030480/1, EP/G030227/1, EP/K01711X/1, EP/K017144/1, EU grants GENIUS and MEM4WIN, a Royal Society Wolfson Research Merit Award, The Royal Academy of Engineering, Emmanuel College and King's College, Cambridge, and an ORSAS scholarship from Heriot-Watt University. RM and SJB acknowledge Prof. D. T. Reid for useful discussions.

#182934 - $15.00 USD Received 7 Jan 2013; revised 10 Mar 2013; accepted 13 Mar 2013; published 25 Mar 2013